

ASSESSMENT OF THE EFFECTS OF THE ACCELERATION PARAMETERS ON THE MAXIMUM INTERNAL FORCES IN THE TUNNEL LININGS AT METRO LINE 3 IN HANOI

Chu Quang Cao¹, Ngoc Anh Vu^{1,*}, Van Hung Nguyen¹

¹*Le Quy Don Technical University, Hanoi, Vietnam*

Abstract

This article presents a method of regression analysis to determine the influence of these parameters on the maximum values of the internal forces in the tunnel structure. In which, the data analysis is the internal forces in the tunnel structure calculated by Plaxis software with different artificial accelerations with same target response spectrum generated by random simulation. The results show that the peak acceleration value is not the only parameter affecting the internal force of the structure, but also some other parameters such as: peak ground velocity, significant time (t_{5-95}), Arias intensity and effective acceleration.

Keywords: *Seismic analysis; segmental lining; artificial acceleration; semi-rigid joint; response spectrum; acceleration parameters.*

1. Introduction

The metro line is an important component of the urban transport system. The underground sections of these lines are often excavated and built by using TBM (Tunnel Boring Machine). Although underground structures have many advantages compared with structures on the surface in case of these structures impacted by seismic waves. In fact, there are many mechanical failures of tunnel in the world under earthquake activities.

The full dynamic analysis of tunnel structures under seismic loads has been studied by many authors [1-7] used numerical analysis techniques to calculate some types of tunnel structures subjected to seismic loads. Because Vietnam has not had many strong earthquakes recorded, the acceleration diagram used in the calculation is mainly artificial acceleration. Some authors have published some results on this issue such as [8, 9].

This study focuses on using the artificial accelerations, that related to Vietnamese National Standards TCVN 9386:2012 [10] to calculate the tunnel structure at Hanoi, a case study in Ba Dinh district. These input accelerations are randomly generated by PG02, a program has been established basing on the Yamamoto's regression equations [11] and response spectrum matching conditions. From the internal forces

* Email: ngocanh.vu@lqdtu.edu.vn

results, using regression analysis to evaluate the relative influence of the characteristic parameters of the time function on the quantities: maximum moment, maximum shear force, respectively appear in the tunnel structure.

2. Numerical analysis for segmental tunnels

2.1. Introductions of project

The object selected for the survey, is the underground section of the project "Urban Railway (Metro) No. 3, Nhon - Hanoi Railway Station". This project has total in length 12.5 km, maintance Depot with slabing area in Nhon with 8.5 km elevated via ductsection and 4 km in twin tube underground tunnel (with 4 underground stations from station S9 to S12, Fig. 1) located at Ba Dinh district. Because the tunnel length is much larger than the other dimensions, it is assumed that the structure modeling is plane deformation problem.



Fig. 1. Plan of Metro line No. 3 in Hanoi City [12].

2.2. Soil properties

Geology from the ground level to bottom has a thickness of 60 m, including 6 geological layers (denoted from L1 to L6). The parameters of each layer are described in Tab. 1. Ground surrounding medium the tunnel is simulated as 15-nodes triangle elements and the Hardening Soil (HS) model is selected. The depth of underground water is 5 m from the ground surface.

Tab. 1. Parameters of soil layers [12]

| Row | Parameters | Denoted | Layers | | | | | |
|-----|---------------------|---------|--------|----|-----|------|------|------|
| | | | 1 | 2 | 3 | 4 | 5 | 6 |
| 1 | Layer thickness (m) | | 2.5 | 15 | 3.5 | 15.0 | 11.0 | 13.0 |

| Row | Parameters | Denoted | Layers | | | | | |
|-----|--|------------------|----------|----------|----------|----------|----------|----------|
| | | | 1 | 2 | 3 | 4 | 5 | 6 |
| 2 | Model materials | | HS | HS | HS | HS | HS | HS |
| 3 | Saturated density (kN/m ³) | γ_{sat} | 18 | 17.8 | 19.4 | 20.0 | 21.0 | 23.0 |
| 4 | Natural density (kN/m ³) | γ_{unsat} | 17 | 16.8 | 19.4 | 20.0 | 21.0 | 23.0 |
| 5 | Oed-stiffness modulus (kPa) | E_{oed}^{ref} | 5,100 | 3,600 | 16,200 | 25,200 | 48,800 | 131,000 |
| 6 | Secant stiffness modulus (kPa) | E_{50}^{ref} | 5,100 | 3,600 | 16,200 | 25,200 | 48,800 | 131,000 |
| 7 | Load-unloading Modulus (kPa) | E_{ur}^{ref} | 1.53E+04 | 1.08E+04 | 4.85E+04 | 7.55E+04 | 1.46E+05 | 3.94E+05 |
| 8 | Poisson's coefficient | ν | 0.3 | 0.35 | 0.30 | 0.30 | 0.30 | 0.28 |
| 9 | Cohesion force (kN/m ²) | c | 55 | 30 | 0.1 | 0.1 | 0.1 | 0.1 |
| 10 | Internal friction angle (°) | ϕ | 20 | 12 | 31 | 37 | 39 | 45 |
| 11 | Interactive coefficient | R_{inter} | 0.8 | 0.8 | 0.7 | 0.7 | 0.7 | 0.7 |

2.3. Properties of segmental tunnel lining

The tunnel is located at depth of 25 meters below the surface. The segmental tunnel structure material in the model is assumed to be homogeneous and satisfy the linear elastic model, cross-section features of tunnel structure are shown in Tab. 2.

Tab. 2. Parameters of tunnel structure in analysis [12]

| Row | Parameters | Denoted | Values | Units |
|-----|--|------------------|---------|-------|
| 1 | Tunnel diameter (internal/outer) | D_{in}/D_{out} | 5.7/6.3 | m |
| 2 | Modulus of elasticity of tunnel concrete | E_b | 2.5E+7 | kPa |
| 3 | Poisson's coefficient | ν | 0.15 | |
| 4 | Thickness of lining | t | 0.30 | m |
| 5 | Height of the connection | l_t | 0.185 | m |
| 6 | Width of the tunnel ring | b | 1.0 | m |

Using Janssen's assumptions [13] to simulate connection among segments of tunnel lining (Fig. 2) where C_r is elastic jointing anti-bending hardness (rotational spring), k_r is the elastic link hardness in the radius direction (radial spring), k_t is the elastic link hardness in the tangentially direction (tangential spring).

The values for k_r and k_t are often chosen with high values, when using Plaxis 2D, these links usually are ignored in calculation. The main parameter of the Janssen joint [13], C_r is determined by formula (1):

$$C_r = \frac{b \cdot l_t^2 \cdot E_c}{12} = \frac{1 \cdot 0.185^2 \cdot 2.5 \cdot 10^7}{12} = 71,302 \text{ (kN.m/rad)} \quad (1)$$

where l_t is the height of the connection (m); E_c is the elastic module of concrete (kN/m²); b is width of the tunnel ring (m).

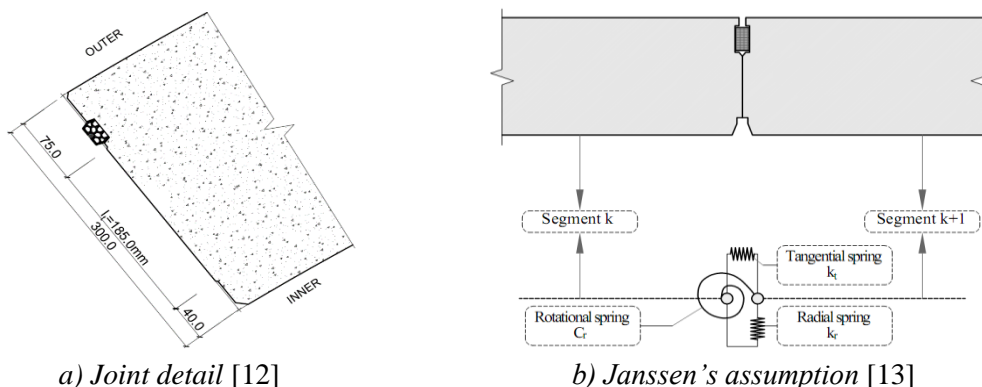


Fig. 2. Joint detail and Janssen's assumption.

The semi-rigid joints are modelled in Plaxis as a 'Hinges and rotation springs', in there, the spring stiffness is C_r value (Fig. 3, Min.Moment = $-M_{yield} = -150$ kN.m; Max.Moment = $M_{yield} = 150$ kN.m [13]).

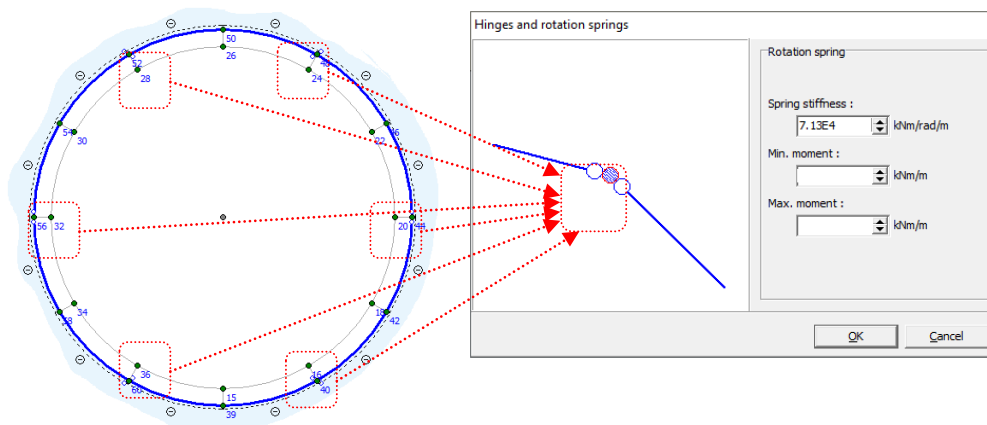


Fig. 3. Semi-rigid joint is modeled in the Plaxis 2D software.

Model of segmental tunnel structure and the 2-dimension plane strain model (with 6 segments) in Plaxis software can be shown in Fig. 4.

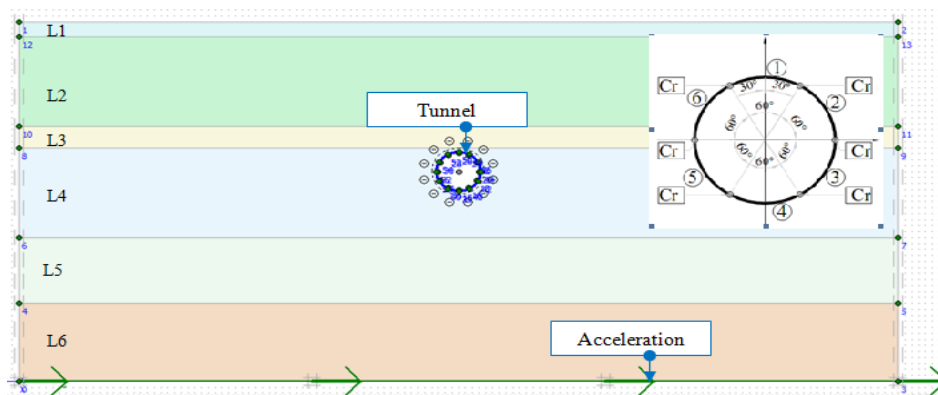


Fig. 4. 2D plane strain model in Plaxis software.

3. Input accelerations and method to evaluate the effect of parameters of acceleration on internal forces of tunnel lining

3.1. Input accelerations

Time history input is artificial accelerations, which is generated by PG02, a program was written on MATLAB. This program is a random simulation method based on Yamamoto's regression equation, randomly generating artificial acceleration with a same target spectrum. The input data provided to the PG02 program includes 2 categories:

- The parameters of the source are determined with the central location of Ba Dinh district, the Red River - Song Chay earthquake zone [14] with: seismic magnitude $M_w = 6.2$; focal depth $R_{hyp} = 17$ km; distance from the survey point to the epicenter $R_{rup} = 11$ km.

- The target spectrum is determined by Vietnamese National Standard TCVN 9386:2012 [10] with Ba Dinh district: the peak reference acceleration: $a_{gR} = 0.0976$ g; the important coefficient: $\gamma_I = 1.0$; site classification: A class.

Using PG02 to generate 18 accelerations (denoted from bd01_01a to bd01_18a), the results are shown in figures from 5 to 22.

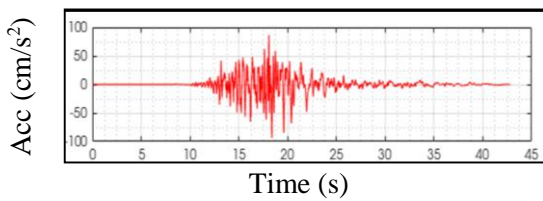


Fig. 5. Acceleration *bd01_01a*.

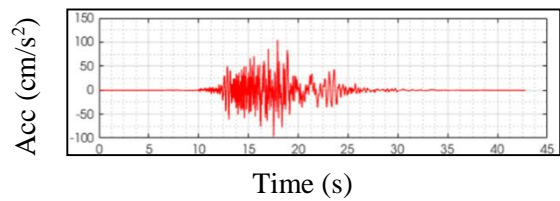


Fig. 6. Acceleration *bd01_02a*.

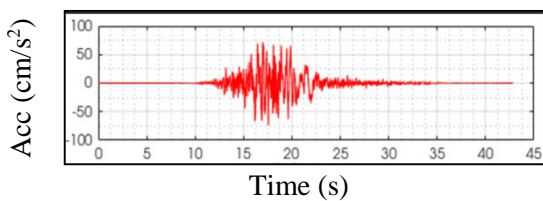


Fig. 7. Acceleration *bd01_03a*.

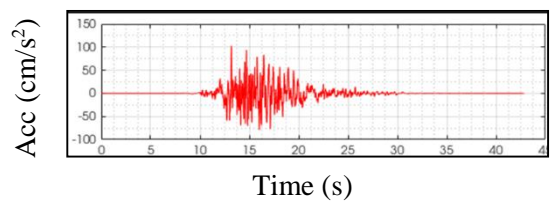


Fig. 8. Acceleration *bd01_04a*.

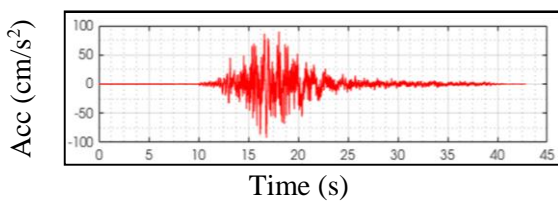


Fig. 9. Acceleration *bd01_05a*.

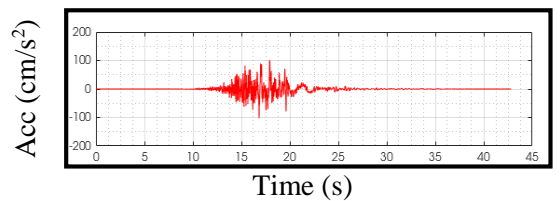


Fig. 10. Acceleration *bd01_06a*.

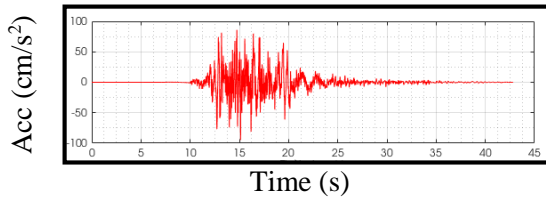


Fig. 11. Acceleration bd01_07a.

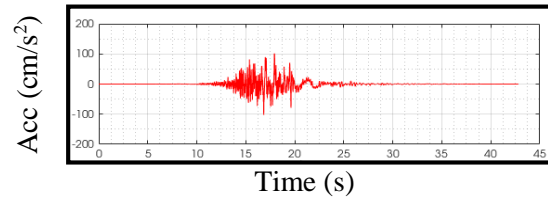


Fig. 12. Acceleration bd01_08a.

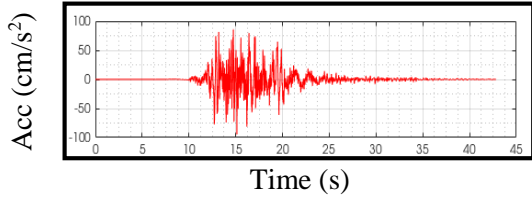


Fig. 13. Acceleration bd01_09a.

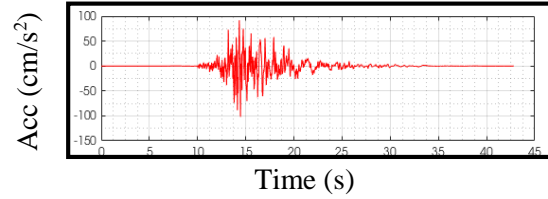


Fig. 14. Acceleration bd01_10a.

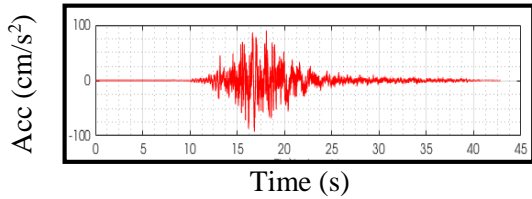


Fig. 15. Acceleration bd01_11a.

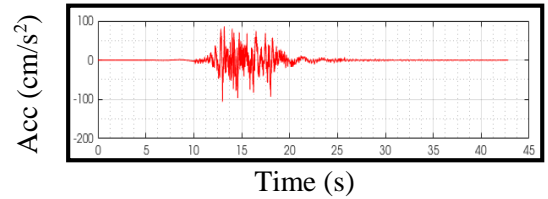


Fig. 16. Acceleration bd01_12a.

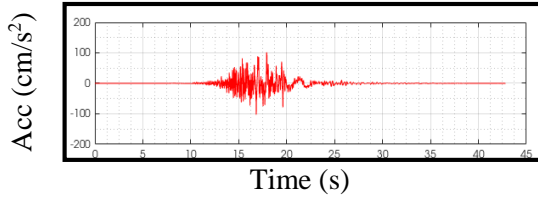


Fig. 17. Acceleration bd01_13a.

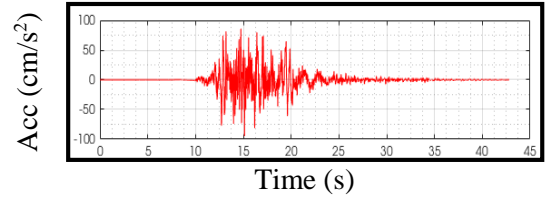


Fig. 18. Acceleration bd01_14a.

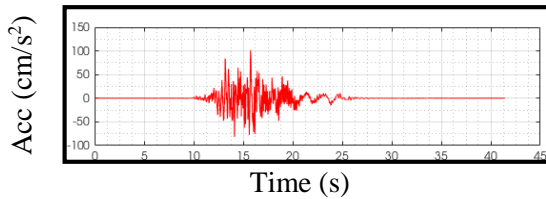


Fig. 19. Acceleration bd01_15a.

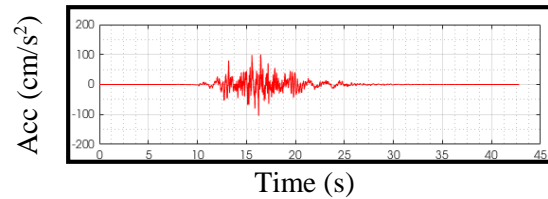


Fig. 20. Acceleration bd01_16a.

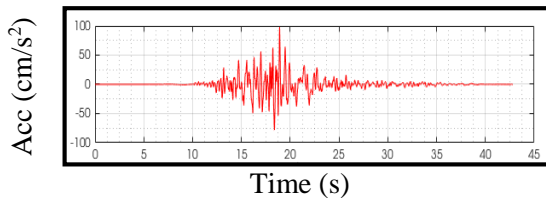


Fig. 21. Acceleration bd01_17a.

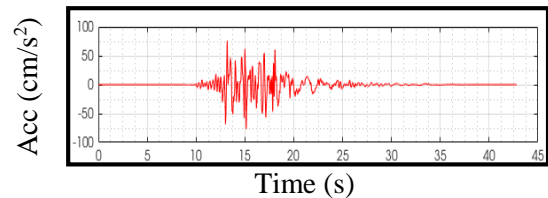


Fig. 22. Acceleration bd01_18a.

The responses of 18 accelerations can be shown in Fig. 23.

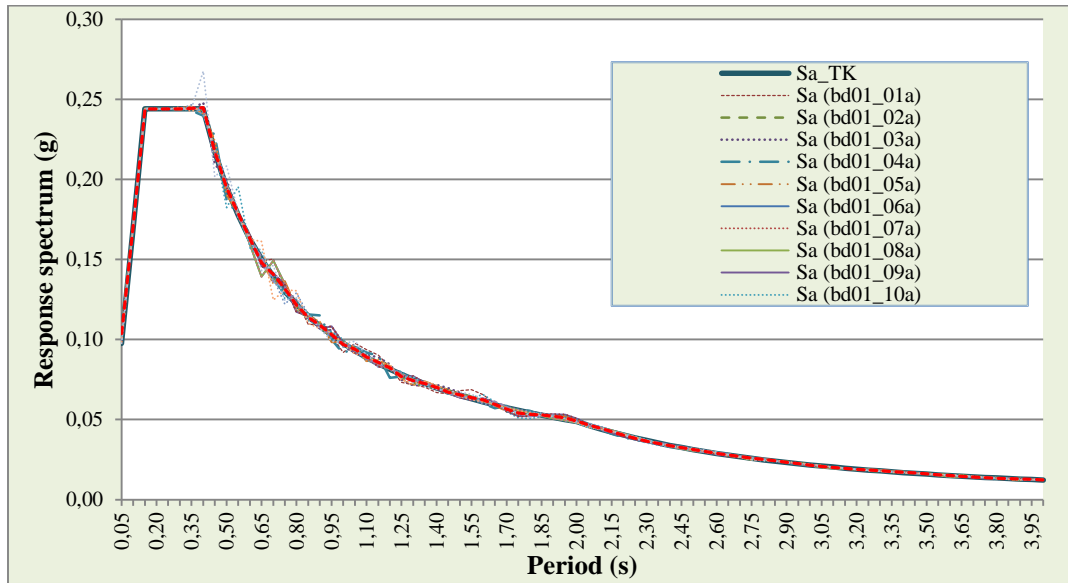


Fig. 23. Response spectrum of 18 artificial accelerations.

3.2. Method to evaluate the effect of parameters of acceleration on internal forces in tunnel lining

In order to determine the influence of the characteristics of the acceleration diagram on the maximum internal force values appearing in the tunnel structure, it is necessary to conduct regression analysis. The tool used for the analysis is the commercial software IBM SPSS (short for Statistical Package for the Social Sciences). IBM SPSS software supports primary data processing and analysis, especially useful in regression and correlation analysis [16]. IBM SPSS provides a sophisticated set of univariate and multivariate analytical techniques and models. In this article, the regression analysis data are including two groups:

- Data of independent variables: peak ground acceleration (PGA), Arias intensity (IA), time duration of strong motion (t_{5-95}), effective acceleration (a_{RMS}) and peak velocity (PGV);

- + PGA and PGV are maximum ground acceleration and velocity, respectively, that occurred during earthquake shaking at a location.

- + The root mean square acceleration a_{RMS} is defined as:

$$a_{RMS} = \sqrt{\frac{1}{t_0} \int_0^{t_0} a^2(t) dt} \tag{2}$$

+ IA is a measure of the strength of a ground motion [10]. It determines the intensity of shaking by measuring the acceleration of transient seismic waves proposed by Chilean engineer Arturo Arias in 1970. It is defined as the time-integral of the square of the ground acceleration:

$$IA(t_0) = \frac{2\pi}{g} \int_0^{t_0} [a(t)]^2 dt \quad (3)$$

where g is the acceleration due to gravity and t_0 is the duration of acceleration $a(t)$.

+ Significant duration (t_{5-95}) is the most common measure of significant duration which is a time interval between 5-95% of IA and denoted by t_{5-95} .

- Dependent variable data: Maximum moment and maximum shear force appear in the structure calculated with the tunnel structures.

4. Results

The maximum of internal forces are shown in Tab. 3.

Tab. 3. The results of max internal forces

| Input acceleration | Parameters of acceleration | | | | | Max. internal forces | | |
|--------------------|----------------------------|------------|---------------------------------------|-----------|-----------------------|-----------------------|------------------|-------------------|
| | PGA (cm/s ²) | PGV (cm/s) | a _{RMS} (cm/s ²) | IA (cm/s) | t ₅₋₉₅ (s) | Bending moment (kN.m) | Shear force (kN) | Normal force (kN) |
| bd01-01a | 93.73 | 6.21 | 25.63 | 10.800 | 9.28 | 138.96 | 105.08 | 765.54 |
| bd01-02a | 104.57 | 6.62 | 25.71 | 12.500 | 10.62 | 135.19 | 102.67 | 764.91 |
| bd01-03a | 73.69 | 6.89 | 27.99 | 9.450 | 6.78 | 138.98 | 105.61 | 765.54 |
| bd01-04a | 102.86 | 6.41 | 30.84 | 12.700 | 7.51 | 138.82 | 103.92 | 766.73 |
| bd01-05a | 92.15 | 8.05 | 27.74 | 10.600 | 7.73 | 140.02 | 106.45 | 766.91 |
| bd01-06a | 102.64 | 7.87 | 30.29 | 9.900 | 6.09 | 138.41 | 104.80 | 769.77 |
| bd01-07a | 94.65 | 7.53 | 29.15 | 11.700 | 7.72 | 138.50 | 105.12 | 768.06 |
| bd01-08a | 102.01 | 5.61 | 27.58 | 9.500 | 7.02 | 134.25 | 101.53 | 763.17 |
| bd01-09a | 105.74 | 7.93 | 32.82 | 10.900 | 5.70 | 142.04 | 105.70 | 769.45 |
| bd01-10a | 101.60 | 6.03 | 27.95 | 9.900 | 7.13 | 135.30 | 102.99 | 765.32 |
| bd01-11a | 104.24 | 6.49 | 26.95 | 9.900 | 7.67 | 136.07 | 103.28 | 767.08 |
| bd01-12a | 98.04 | 6.31 | 24.89 | 8.900 | 8.06 | 137.16 | 103.67 | 764.33 |
| bd01-13a | 76.83 | 6.86 | 28.99 | 12.200 | 8.16 | 140.42 | 106.26 | 764.62 |
| bd01-14a | 93.59 | 7.54 | 28.95 | 11.000 | 7.36 | 140.31 | 106.08 | 765.56 |

| Input acceleration | Parameters of acceleration | | | | | Max. internal forces | | |
|--------------------|----------------------------|-------------|---------------------------------------|--------------|-----------------------|-----------------------|------------------|-------------------|
| | PGA (cm/s ²) | PGV (cm/s) | a _{RMS} (cm/s ²) | IA (cm/s) | t ₅₋₉₅ (s) | Bending moment (kN.m) | Shear force (kN) | Normal force (kN) |
| bd01-15a | 88.56 | 8.31 | 28.85 | 9.500 | 6.43 | 136.96 | 103.17 | 768.53 |
| bd01-16a | 101.51 | 7.24 | 29.54 | 14.400 | 9.28 | 138.60 | 103.55 | 769.30 |
| bd01-17a | 99.88 | 8.18 | 30.89 | 10.200 | 5.98 | 142.33 | 107.34 | 769.57 |
| bd01-18a | 76.57 | 7.84 | 25.85 | 8.600 | 7.25 | 136.40 | 102.27 | 764.63 |
| Mean | 95.16 | 7.11 | 28.37 | 10.70 | 7.54 | 138.26 | 104.42 | 766.61 |

Analysis by IBM SPSS [16], through regression coefficient, evaluates the relative influence of the acceleration parameters on maximum moment and maximum shear force, respectively is shown in Fig. 24 and 25 (the level of influence expressed in percentage).

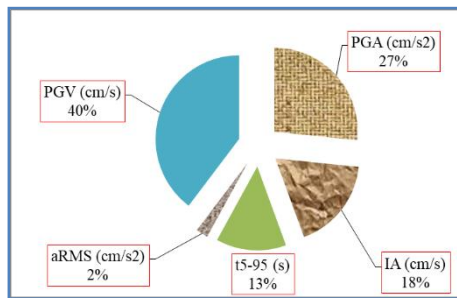


Fig. 24. Effect of acceleration parameters on max. bending moment.

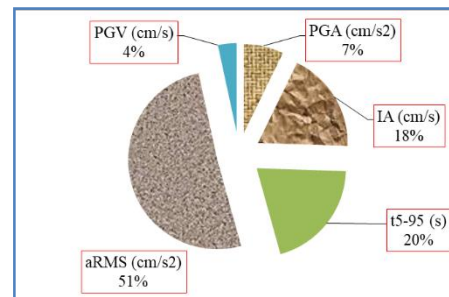


Fig. 25. Effect of acceleration parameters on max. shear forces.

5. Conclusion

By above researches, some conclusions can be drawn:

- PGV and PGA significantly affect the moment and axial force values, however they have a small effect on the shear force value.
- Features such as IA and significant duration t_{5-95} have a noticeable influence on maximum internal forces appearing in the tunnel structure.

The new research results only stop at a small number of results in the case of specificity. To draw more in-depth conclusions, multiple analyzes with a large number of trials in follow-up studies are required.

References

- [1] Brinkgreve R.B.J. and Broere W., *Plaxis manual version 8*, Delft University of technology & Plaxis b.v., The Netherlands, 2006.
- [2] Kontoe, S., Zdravkovic, L., Potts, D.M. and Menkiti, C.O., "Case study on seismic tunnel response," *Canadian Geotechnical Journal*, 45, pp. 1743-1764, 2008.
- [3] Youssef M.A. Hashash, Jeffrey J. Hook, Birger Schmidt, John I-Chiang Yao, "Seismic design and analysis of underground structures," *Tunnelling and Underground Space Technology*, 16, pp. 247-293, 2001.
- [4] St. John, C.M., Zahrah, "A seismic design of underground structures," *Tunnelling Underground Space Technol.*, 2 (2), pp. 165-197, 1987.
- [5] ITA WG research, "Guidelines for the design of shield tunnel lining," *Tunnelling and Underground Space Technology*, Vol. 15, 2000.
- [6] Do, N.A. "Numerical Analyses of segmental tunnel lining under static and dynamic loads," Ph.D. thesis, 2014.
- [7] Vu, N.A., Cao, C.Q. and Nguyen, V.H. "Calculation of tunnel linings under seismic loads of the earthquakes by generated the artificial acceleration applied in the Ha Noi area," *Section on Special Construction Engineering/Journal of Science and Technique*, Vol. 3, No. 1, 2020.
- [8] Nguyen, X.D. and Nguyen, V.T., "A proposed method for selecting and scaling recorded seismic accelerations according to TCVN 9386:2012," *Journal of Science and Technology in Civil Engineering (STCE) - HUCE*, 16(1), pp. 100-112, 2022.
- [9] Vu, N.A. and Cao, C.Q., "A seismic analysis of segmental tunnel lining using artificial acceleration," *Section on Special Construction Engineering/Journal of Science and Technique*, Vol. 4, No. 2, 2021.
- [10] *Thiết kế công trình chịu động đất*, Tiêu chuẩn Việt Nam TCVN 9386:2012.
- [11] Yamamoto, "Stochannstic model for earthquake ground motion using Wavelet packets," Ph.D. thesis, Stanford University, 2011.
- [12] Design Technical Report, Project: Ha Noi Metro Rail System Project (Line 3: Nhon-Ha Noi Station Section), 2013.
- [13] Janssen, P., *Tragverhalten von Tunnelausbauten mit Gelenktübbings*, "Load carrying behavior of segmented tunnel linings," Ph.D. thesis. Technische Universität Carolo-Wilhelmina zu Braunschweig, Braunschweig (in German), 1983.
- [14] Kramer S.L., *Geotechnical Earthquake Engineering*, Prentice Hall, New Jersey, 1996.
- [15] Nguyễn Ngọc Thủy, Nguyễn Minh Sinh, *Nghiên cứu bổ sung và hoàn chỉnh bản đồ phân vùng nhỏ động đất thành phố Hà Nội mở rộng, tỷ lệ 1:25.000, lập cơ sở dữ liệu về đặc trưng dao động nền đất ở Hà Nội ứng với bản đồ trên*, Sở Xây dựng Hà Nội, 2004.
- [16] Sabine Landau and Brian S. Everitt, *A Handbook of Statistical Analyses using IBM SPSS*, Chapman & Hall/CRC Press LLC, 2004.

ĐÁNH GIÁ ẢNH HƯỞNG CỦA CÁC THAM SỐ GIA TỐC NỀN ĐẾN NỘI LỰC CỰC ĐẠI XUẤT HIỆN TRONG VỎ HÀM CHỊU ĐỘNG ĐẤT TẠI TUYẾN ĐƯỜNG SẮT ĐÔ THỊ SỐ 3 TẠI HÀ NỘI

Cao Chu Quang¹, Vũ Ngọc Anh¹, Nguyễn Văn Hùng¹

¹Đại học Kỹ thuật Lê Quý Đôn, Hà Nội, Việt Nam

Tóm tắt: Bài báo trình bày phương pháp phân tích hồi quy để xác định vai trò ảnh hưởng của các đặc trưng này đến giá trị nội lực cực đại xuất hiện trong kết cấu vỏ hầm. Trong đó, số liệu phân tích là nội lực xuất hiện trong kết cấu được tính toán bằng phần mềm Plaxis với các giản đồ gia tốc khác nhau nhưng có cùng phổ phản ứng mục tiêu được tạo ra bởi mô phỏng ngẫu nhiên. Kết quả bài toán cho thấy: giá trị gia tốc đỉnh không phải là yếu tố duy nhất ảnh hưởng đến nội lực của kết cấu các đặc trưng như vận tốc nền cực đại, thời gian duy trì dao động mạnh t_{5-95} , cường độ Arias và gia tốc hiệu dụng đều có ảnh hưởng nhất định đến nội lực cực đại xuất hiện trong kết cấu.

Từ khóa: Tính toán công trình chịu động đất; vỏ hầm lắp ghép; giản đồ gia tốc nền nhân tạo; liên kết nửa cứng; phổ phản ứng đàn hồi; các tham số của gia tốc nền.

Received: 15/09/2022; Revised: 12/12/2022; Accepted for publication: 30/12/2022

